

MID-INFRARED SPECTROSCOPY OF HIGH REDSHIFT SUBMILLIMETER GALAXIES: FIRST RESULTS

KARÍN MENÉNDEZ-DELMESTRE¹, ANDREW W. BLAIN¹, DAVE M. ALEXANDER², IAN SMAIL², LEE ARMUS³, SCOTT C. CHAPMAN^{4,5}, DAVE FRAZER³, ROB J. IVISON^{6,7}, HARRY TEPLITZ³

Draft version December 24, 2018

ABSTRACT

We present mid-infrared spectra of 5 submm galaxies at redshifts $z = 0.65 - 2.38$ taken with the *Spitzer Space Telescope*. Four of these sources have strong PAH features and their composite spectrum is well fitted by an M82-like spectrum with an additional less-intense AGN power-law component, $F_\nu \sim \nu^{1.6}$. Comparison with local templates of both the 7.7- μm PAH feature equivalent width and PAH-to-infrared luminosity ratio is consistent with these galaxies being hosts to both star-formation and AGN activity, with star-formation dominating the bolometric luminosity. The other source displays a Mrk 231-type broad emission feature at restframe $\sim 8\mu\text{m}$ that does not conform to the typical 7.7/8.6 μm PAH complex in starburst galaxies, suggesting a more substantial AGN contribution.

Subject headings: infrared: galaxies – galaxies: starburst – galaxies: AGN – technique: spectroscopic

1. INTRODUCTION

In the past decade, deep submillimeter-wave surveys (Smail et al. 1997; Barger, Cowie & Sanders 1999; Eales et al. 1999; Cowie et al. 2002; Scott et al. 2002; Borys et al. 2003; Webb et al. 2003b) have uncovered a population of highly obscured, ultra-luminous infrared (IR) galaxies (ULIRGs; $L_{\text{IR}} > 2 - 5 \times 10^{12} L_\odot$) at $z \sim 2$ (Blain et al. 2002). These submillimeter galaxies (SMGs) represent a significant population of galaxies at the epoch of peak global star formation and quasar activity. However, highly obscured by their dust content, the astrophysics of SMGs and the nature of their power source remain a challenge to address at optical and near-IR wavelengths (Chapman et al. 2003, 2005, hereafter C05; Swinbank et al. 2004). X-ray evidence indicates that $\sim 28 - 50\%$ of SMGs host an active galactic nucleus (AGN), although at face value it appears that the AGN contribution does not dominate the bolometric luminosity and that powerful starbursts (SB) contribute more significantly to the total energy output (Alexander et al. 2005, hereafter A05).

Less hindered by obscuration than shorter wavelengths, the mid-IR region boasts a number of spectral features whose strengths vary according to the nature of the dominant energy source in the galaxy. These features include: emission from Polycyclic Aromatic Hydrocarbons (PAHs) (e.g. restframe 6.2, 7.7, 8.6, 11.3 and 12.7 μm), associated with star formation (SF) (Helou 1999) and typically absent in powerful AGN (Voit 1992); strong silicate absorption at 9.7 and 18 μm , which gives a measure of the obscuration by silicate dust grains along

the line of sight to a small hot dust continuum source; and a hot dust continuum, likely to be dominated by an AGN. The strength of these features have been used in mid-IR surveys with the *Infrared Space Observatory* (Genzel et al. 1998; Rigopoulou et al. 1999; Tran et al. 2001) to estimate the relative contributions from SF and AGN activity, but only for the brightest local galaxies (e.g. Rigopoulou et al. 1999). The high-redshift population remained unexplored in the mid-IR, until the advent of the *Spitzer Space Telescope*. The unprecedented sensitivity of the Infrared Spectrograph (IRS; Houck et al. 2004) on *Spitzer* allows us today to observe mid-IR spectra of galaxies out to $z \sim 3$. Lutz et al. (2005) and Yan et al. (2005), hereafter L05 and Y05, together with Houck et al. (2005), Desai et al. (2006) and Weedman et al. (2006) have been among the pioneers in using IRS to investigate the mid-IR spectra of ULIRGs at $z \sim 1 - 3$, expanding to higher redshifts the analysis that was previously only accessible for nearby, bright galaxies.

We are undertaking an IRS program to study the range of mid-IR properties of a sample of 26 high- z SMGs, using the radio-identified sample with spectroscopic redshifts, compiled by C05. These galaxies require long integration times to obtain spectra with good signal-to-noise ratio (S/N). To optimize their detection within reasonable integration times, we selected our targets from the bright end of the C05 sample, with $S_{24\mu\text{m}} \gtrsim 0.4 \text{ mJy}$. Here we present IRS spectra observed early in our program. Four of the targets are at lower- z , with $z = 0.65 - 1.5$, and one is at $z \sim 2.38$. The low- z targets provide wavelength coverage longwards of 10 μm and give insight into the longer mid-IR emission from SMGs; the full sample is otherwise more focused on $z \sim 2$ SMGs and hence probes shorter restframe wavelengths.

2. OBSERVATIONS AND REDUCTION

We observed each target using the low resolution Long-Low (LL) observing mode of IRS ($R \sim 57 - 126$) at two different nod positions for 30 cycles of 120s each. We cover restframe emission longwards of 6 μm to probe for PAH emission at 6.2, 7.7, 8.6 and 11.3 μm and for silicate absorption centered at 9.7 μm . The data were obtained

¹ California Institute of Technology, MC 105-24, Pasadena, CA 91125

² Institute for Computational Cosmology, Durham University, Durham DH1 3LE, UK

³ Spitzer Science Center, MC 220-6, California Institute of Technology, Pasadena, CA 91125

⁴ Institute of Astronomy, Madingley Road, Cambridge, CB3 0HA, U.K.

⁵ CSA Fellow, U. of Victoria, Victoria BC, V8P 1A1 Canada

⁶ UK Astronomy Technology Centre, Blackford Hill, Edinburgh EH9 3HJ

⁷ Institute for Astronomy, Blackford Hill, Edinburgh EH9 3HJ
 Electronic address: km@astro.caltech.edu

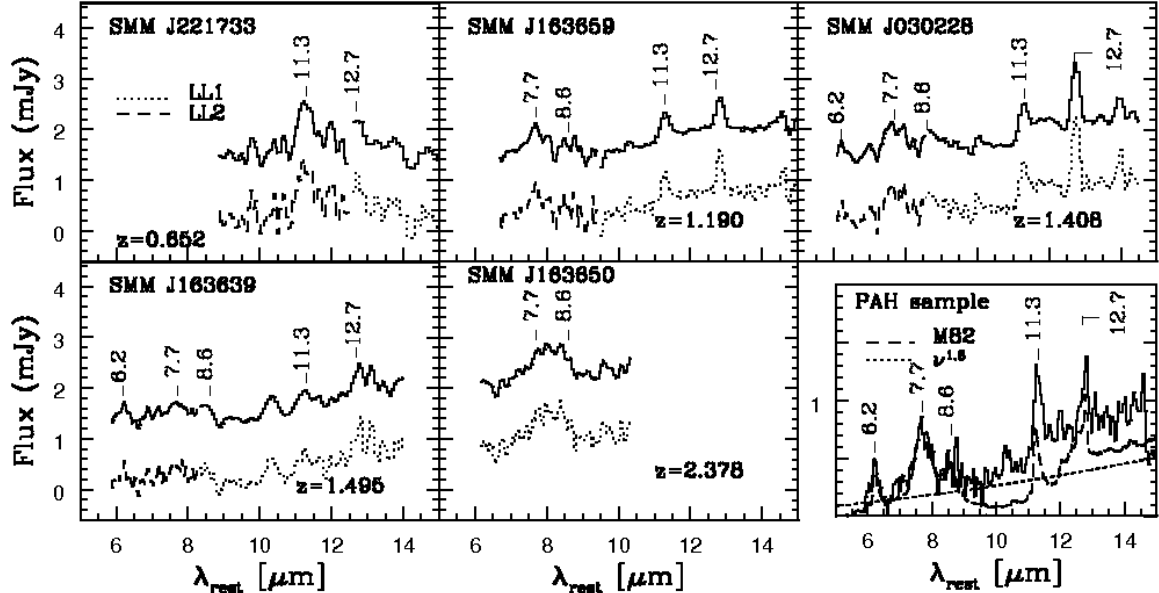


FIG. 1.— 1D *Spitzer* IRS spectra for 5 SMGs and the composite spectrum of the PAH sample. For the individual spectra, the lower curve represents the unsmoothed spectrum at observed flux, with the first order (LL1: $\lambda_{obs} = 19.5 - 38 \mu\text{m}$) and second order (LL2: $\lambda_{obs} = 14 - 21.3 \mu\text{m}$) of the low-resolution mode shown in dotted and dashed lines, respectively. The upper curve shows the spectrum smoothed by 3 pixels and offset in flux for clarity. PAH emission features are indicated at the various restframe wavelengths. We show the smoothed version of the composite spectrum for the PAH sample, together with the ISO SWS spectra of M82 (dashed line), smoothed to the resolution of IRS for comparison and normalized to the 7.7- μm PAH feature. The excess in the SMG composite, when fitted by M82, is consistent with emission from an AGN (see §3.1.2). The additional power-law component is shown by the dotted line (see text).

between December 2005 and March 2006.

The data were processed using the Spitzer IRS S13 pipeline⁸, which includes saturation flagging, dark subtraction, linearity correction, ramp correction and flat-fielding. With a slit size of $\sim 10.5 \times 168''$, IRS does not resolve the SMGs spatially, and the targets were treated as point sources throughout the data reduction and analysis. We performed additional reduction of the 2D spectra using IRSCLEAN⁹ to remove rogue pixels, and relied on differencing between the nod positions to subtract the residual background. We used the SPitzer IRS Custom Extraction (SPICE)¹⁰ software to optimally extract flux-calibrated 1D spectra, by taking a weighted average of profile-normalized flux at each wavelength to increase the S/N in IRS observations of faint sources. Our first 5 targets are SMM J221733 +001120, SMM J163659 +405728, SMM J030228 +000654, SMM J163639 +405636, and SMM J163650 +405735. The spectra are shown in Fig. 1.

3. RESULTS AND DISCUSSION

The mid-IR spectra of SMM J221733, SMM J163659, SMM J030228 and SMM J163639 show moderate to strong PAH features, and we refer to these targets collectively as the *PAH sample*. Detection of PAH emission is assumed to indicate the presence of SF activity. At most a very shallow dip is present around 9.7 μm in the spectra, indicating little silicate absorption.

Our highest- z source, SMM J163650, is somewhat different to the other targets, with a broad emission feature at restframe $\sim 8 \mu\text{m}$, unlike the typical blended PAH complex of the 7.7- and 8.6- μm features found in SB

galaxies. It is more reminiscent of Mrk 231 (Armus et al. 2006b, hereafter A06b), which has an unabsorbed continuum between two absorption features, due to silicates at longer wavelengths and hydrocarbons at shorter ones (Spoon et al. 2004, hereafter S04; Weedman et al. 2006). This similarity suggests that SMM J163650 has more substantial AGN-activity than the SMGs in the PAH sample, as expected from the presence of a strong CIV ($\lambda 1549$) feature at restframe UV (C05) and a broad-line H α component ($\text{FWHM} \simeq 1753 \pm 238 \text{ km s}^{-1}$; see Swinbank et al. 2004), both revealing the unambiguous presence of an AGN. We discuss the properties of this source in more detail in a subsequent paper discussing the full sample (Menéndez-Delmestre et al. in prep.) and concentrate here on the median properties of the SMGs with clear PAH emission.

To get an insight into the physics inherent to SMGs in our PAH sample, we compare their spectra with a number of extensively studied local templates: the AGNs Mrk 231 (A06b) and NGC 1068 (Sturm et al. 2000), the SB M82 (Förster Schreiber et al. 2003) and the well-studied ULIRGs Arp 220 (A06b) and NGC 6240 (Armus et al. 2006a, hereafter A06a). Arp 220 has been a favorite template for high-redshift SMGs (C05, Pope et al. 2006): it has strong PAH features, indicative of SB activity, and a steep mid-IR continuum due to a heavily obscured nuclear component inferred to be responsible for the bulk of the IR luminosity (S04). On the other hand, NGC 6240 is a system where AGNs have been identified in both merging components but in which SF dominates the total IR luminosity (Komossa et al. 2003).

A qualitative comparison of the spectra of our PAH sample with these templates rules out Mrk 231,

⁸ <http://ssc.spitzer.caltech.edu/irs/dh/>

⁹ <http://ssc.spitzer.caltech.edu/archanaly/contributed/irsclean>

¹⁰ <http://ssc.spitzer.caltech.edu/postbcd/spice.html>

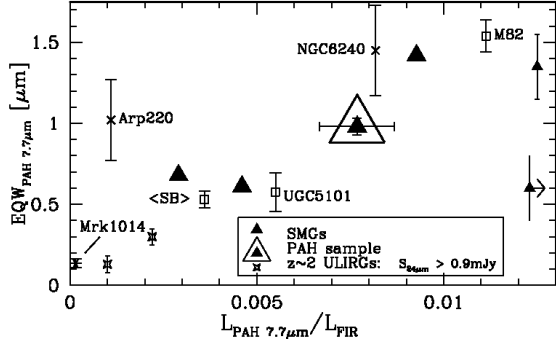


FIG. 2.— Relative strengths of the 7.7- μm PAH feature as measured by the PAH-to-IR (8 – 1000 μm) and the restframe EW. The error in $L_{7.7\mu\text{m}}/L_{\text{IR}}$ for our SMG sample (large triangles) is dominated by a $\simeq 20\%$ uncertainty in the IR luminosities, which were taken from C05 and Kovács et al. (2006). Error bars for the Y05 sources, for the SB-dominated UGC 5101 (Armus et al. 2004) and for the average of 13 nearby SB galaxies studied with IRS (Brandl et al. 2006) reflect the uncertainty in the values as presented by the authors of the respective papers. We estimate the values for M82 (Förster Schreiber et al. 2003), Arp 220 (S0), NGC 6240 (A06a) and for the L05 pair of SMGs (small triangles) directly from their published spectra assuming a linear continuum slope; the error bars reflect the uncertainties of this approach. Due to differences in continuum definition, the EW for NGC 6240 shown here is lower than that presented by A06a, where they performed a detailed decomposition of the IR continuum into different temperature components.

NGC 1068 and Arp 220 as good matches, but the spectra are similar to those of M82 and NGC 6240. Similar results were found by L05, who detected strong PAH features in the spectra of two luminous SMGs at $z \sim 2.8$ that were well fitted by an M82-type spectrum.

3.1. The Composite SMG spectrum

We double the S/N of the individual spectra by taking advantage of the similarity in the mid-IR spectra of the PAH sample and constructing a composite spectrum. The composite spectrum allows us to address better the nature of the power source and to make a preliminary assessment of the independent contributions of SF and AGN activity in our PAH sample. We emphasize that with our precise known redshifts (C05) it is straightforward to produce a composite spectrum, shown in Fig. 1, by averaging the individual spectra.

Normalizing the local templates to the 7.7- μm peak in the composite spectrum, we find that the composite spectrum is well fitted at wavelengths shortward of $\lambda \simeq 9\mu\text{m}$ by the NGC 6240 and M82 spectra (Fig. 1). However, neither template provide a good characterisation of the composite spectrum longwards of $9\mu\text{m}$: the continuum emission of NGC 6240 exceeds that of the composite spectrum longwards of $12\mu\text{m}$, while the spectrum of M82 falls below it. No physically reasonable additional AGN component can be added to the NGC 6240 spectrum to produce a good fit to the composite spectrum at longer wavelengths. On the other hand, an M82-type spectrum plus a power-law continuum provides a good fit to the composite SMG data at all wavelengths.

3.1.1. Starburst Component

The restframe 7.7- μm PAH feature is generally the most prominent in the mid-IR spectra of SB galaxies.

Its strength relative to the continuum, measured by the equivalent width, $\text{EW}_{7.7\mu\text{m}}$, can be used as a diagnostic to evaluate the fractional contribution of SF to the total bolometric output by comparison with local templates, as the mid-IR continuum is enhanced significantly in the presence of an AGN. SB-dominated objects, such as M82 and NGC 6240, are characterized by larger PAH EWs than objects with a prominent AGN, such as Mrk 231.

The EW is sensitive to how the continuum is defined. We define a linear continuum by interpolating between two points clear of PAH emission features, at $\sim 6.8\mu\text{m}$ and $\sim 13.7\mu\text{m}$, or $\sim 9\mu\text{m}$ when the spectrum does not include one of these points. In Fig. 2, we plot the 7.7- μm restframe EWs and PAH-to-IR luminosity ratios for those SMGs in our sample with a 7.7- μm PAH detection and for the composite spectrum of the PAH sample. We also show a number of low- and high- z sources, including 2 ULIRGs at $z \sim 2$ with clear PAH detections from the 24 μm -bright Y05 sample ($S_{24\mu\text{m}} \gtrsim 0.9\text{ mJy}$), and 2 bright SMGs (SMM J02399–0136 with $S_{850\mu\text{m}} = 23\text{ mJy}$ and MM J154127+6616 with $S_{850\mu\text{m}} = 14.6\text{ mJy}$) at $z \simeq 2.8$ presented by L05.

According to the line-to-continuum (l/c) diagnostic presented by Genzel et al. (1998), systems with $(\text{l/c})_{7.7\mu\text{m}} \gtrsim 1$ are classified as SB-dominated and those with $(\text{l/c})_{7.7\mu\text{m}} < 1$, as AGN-dominated. With $(\text{l/c})_{7.7\mu\text{m}} \gtrsim 1$, SF appears to dominate in the Y05 sample and in the SMGs of both L05 and our PAH sample¹¹. However, the distribution in 7.7- μm EW and PAH-to-IR luminosity ratio in Fig. 2 may suggest a distinction in the relative SF-to-AGN contributions for these three samples, with lower values of these parameters indicating a stronger AGN contribution. We distinguish three regions in Fig. 2: (1) a region with low PAH-to-IR luminosity ratios, occupied by Mrk 1014 (Armus et al. 2004) and the 24 μm -bright sample of Y05; (2) an intermediate PAH-to-IR luminosity region where NGC 6240 and the bulk of the SMGs in our sample are located; and (3) a region with the highest PAH-to-IR luminosity ratios, occupied by M82 and the two SMGs in L05.

At $z \sim 2$, 24- μm flux traces 8- μm restframe continuum; a stronger mid-IR continuum (produced by an AGN) dilutes the strength of PAH features, leading to lower $L_{7.7\mu\text{m}}/L_{\text{IR}}$. The location of the Y05 sample in the plot could follow from the selection of 24 μm -bright targets ($S_{24\mu\text{m}} \gtrsim 0.9\text{ mJy}$) at this redshift, which would bias the selection to objects with lower SF-to-AGN ratios. SMGs in our sample have higher $L_{7.7\mu\text{m}}/L_{\text{IR}}$ ratios, similar to NGC 6240, which we interpret as an indication of a SF contribution to the total luminosity markedly stronger than that of the Y05 sample. At similar IR luminosities, the L05 SMG pair has even higher $L_{7.7\mu\text{m}}/L_{\text{IR}}$, particularly in the case of SMM J02399–0136, for which earlier CO studies have suggested the presence of substantial SF (Frayer et al. 1998). The L05 pair of SMGs appear to be systematically even more SB-like than our sample. This difference could be due to the selection by L05 of SMG targets with markedly greater submm fluxes for similar 24 μm -fluxes, indicating substantially greater IR-luminosities for similar hot dust continua, leading to expected lower contributions from AGN activity.

The SMGs in our PAH sample have values of $\text{EW}_{7.7\mu\text{m}}$

¹¹ For our sample, $(\text{l/c}) \sim 1$ corresponds to $\text{EQW} \sim 0.5\mu\text{m}$

and $L_{7.7\mu\text{m}}/L_{\text{IR}}$ that place their SF-to-AGN ratio between that of the AGN-dominated ULIRG Mrk 1014 and the SB M82. This is qualitatively similar to NGC 6240, which has both SB and AGN components. As a caveat, we note that even though the 7.7- μm PAH-to-FIR luminosity ratio is associated to the SF-to-AGN ratio, it is also sensitive to details of the spectral energy distribution of the system, such as the presence of multiple dust components at different temperatures and the amount of extinction (e.g. Arp 220; S04).

3.1.2. The AGN Component

Mid-IR line diagnostics suggest that SMGs are SB-like. The spectra of both SB-dominated galaxies M82 and NGC 6240 provide a good fit to the composite spectrum at wavelengths shortward of $\simeq 9\mu\text{m}$. However, only an M82-type spectrum with an additional power law AGN component gives a good fit to the composite spectrum at all wavelengths, where the power law is given by $S_\nu \sim \nu^{1.6}$ and where the spectral index, $\alpha = 1.6$, is consistent with the distribution of IR spectral indices for 3C quasars in Simpson & Rawlings (2000). To explore the contribution of this AGN component, we inspect the residuals obtained by subtracting a best fitting M82-type fit from the SMG composite spectrum.

From the residual flux at $10.5\mu\text{m}$ we estimate the X-ray luminosity (L_X) using the correlation between $S_{10.5\mu\text{m}}$ and $S_{2-10\text{keV}}$ presented by Krabbe et al. (2001). This yields $L_X \sim 10^{44}\text{ erg s}^{-1}$ for an AGN at the average redshift for the SMGs presented in this paper, $z \sim 1.4$, in reasonable agreement with the X-ray luminosities found for the SMGs in A05. The residual flux is consistent with an underlying AGN which contributes of order $\sim 10\%$ of the total IR emission. This agrees with the A05 result that AGN activity is often present in SMGs but does not appear to dominate the energetics.

As a caveat, we caution that due to the small number of objects included in the composite, the agreement between the predicted X-ray luminosity due the IR excess and the typical X-ray luminosity of the SMGs in A05 may be fortuitous. Since the $10\mu\text{m}$ excess is dominated by lower redshift sources, further SMGs at $z \lesssim 2$,

included in Menéndez-Delmestre et al. (in prep), will better constrain this excess.

4. CONCLUSIONS

We discuss results on the first five targets obtained as part of a *Spitzer* program to characterize the mid-IR spectra of high redshift submm galaxies. In the mid-IR, we are relatively immune to the effects of obscuration at optical and X-ray wavelengths, thus providing a clear view of the physical nature of the power source in SMGs.

We identify moderate to strong PAH features in the majority of our targets and a Mrk 231-type broad emission feature at restframe $\sim 8\mu\text{m}$ in one source. For the SMGs with a detection of the 7.7- μm PAH feature, we evaluate the starburst-to-AGN ratio using the 7.7- μm equivalent widths and PAH-to-IR luminosity ratios as mid-IR diagnostics. We find that SMGs have a starburst mid-IR spectra more like M82 than like Arp 220, which is often quoted as the favorite local analog to high-redshift SMGs. The composite spectrum from the SMGs with PAH features in our sample is well fitted by an M82-like starburst-component with a power-law continuum representing a fainter underlying AGN component. These results provide further evidence that SMGs host both star-formation and AGN activity, but that star-formation appears to dominate the bolometric luminosity, reiterating the role of SMGs as the sites where a significant fraction of the stellar content we see today built up.

We thank the Spitzer Science Center staff for their support, particularly Patrick Ogle for his help in the optimization of the spectral extraction. AWB thanks the Research Corporation and the Alfred P. Sloan Foundation. DMA and IRS acknowledge support from the Royal Society. This work is based [in part] on observations made with the Spitzer Space Telescope, which is operated by the Jet Propulsion Laboratory, California Institute of Technology under a contract with NASA. Support for this work was provided by NASA through an award issued by JPL/Caltech.

REFERENCES

Alexander, D. M., Bauer, F. E., Chapman, S., Smail, I., Blain, A., Brandt, W. N., Ivison, R. 2005, ApJ, 632, 736 (A05)
 Armus, L. et al. 2004, ApJS, 154, 178
 Armus, L. et al. 2006, ApJ, 640, 204 (A06a)
 Armus, L. et al. 2006, ApJ, astro-ph/0610218 (A06b)
 Barger, A. J., Cowie, L. L., & Sanders, D. B. 1999, ApJ, 518, L5
 Blain, A., Smail, I., Ivison, R., Kneib, J.-P., Frayer, D. T. 2002, Phys. Rep., 369, 111B
 Borys, C., Chapman, S., Halpern, M., & Scott, D. 2003, MNRAS, 344, 385
 Brandl, B. R. et al. 2006, ApJ, astro-ph/0609024
 Chapman, S., Blain, A., Ivison, R., Smail, I. 2005, Nature, 422, 695
 Chapman, S., Blain, A., Smail, I., Ivison, R. 2005, ApJ, 622, 772 (C05)
 Cowie, L. L., Barger, A. J., & Kneib, J.-P. 2002, AJ, 123, 2197
 Desai, V. et al. 2006, ApJ, 641, 133
 Eales, S., Lilly, S., Gear, W., Dunne, L., Bond, J.R., Hammer, F., Le Fèvre, O., & Crampton, D. 1999, ApJ, 515, 518
 Förster Schreiber, N. M., Sauvage, M., Charmandaris, V., Laurent, O., Gallais, P., Mirabel, I. F., Vigroux, L. 2003, A&A, 399, 833
 Frayer, D. T., Ivison, R., Scoville, N. Z., Yun, M., Evans, A. S., Smail, I., Blain, A., Kneib, J.-P. 1998, ApJ, 506, L7
 Genzel, R. et al. 1998, ApJ, 498, 579
 Helou, G. 1999, "The Universe as Seen by ISO". Eds. P. Cox & M. F. Kessler. ESA-SP 427., 797
 Houck, J. R. et al. 2004 ApJS, 154, 18
 Houck, J. R. et al. 2005 ApJ, 622, 105
 Komossa, S., Burwitz, V., Hasinger, G., Predehl, P., Kaastra, J. S., Ikebe, Y. 2003 ApJ, 582, 15
 Kovács, A., Chapman, S., Dowell, C. D., Blain, A., Ivison, R., Smail, I., Phillips, T. G. 2006, ApJ, 650, 592
 Krabbe, A., Böker, T., Maiolino, R. 2001 ApJ, 557, 626
 Lutz, D., Valiante, E., Sturm, E., Genzel, R., Tacconi, L., Lehnert, M., Sternberg, A., Baker, A. 2005 ApJ, 625, 83 (L05)
 Pope, A. et al. 2006, MNRAS, 370, 1185
 Rigopoulou, D., Spoon, H. W. W., Genzel, R., Lutz, D., Moorwood, A. F. M., Tran, Q. D. 1999, AJ, 118, 2625
 Scott, S. et al. 2002, MNRAS, 331, 817
 Simpson, C., Rawlings, S. 2000, MNRAS, 317, 1023
 Smail, I., Ivison, R., Blain, A. 1997, ApJ, 490L, 5S
 Spoon, H. W. W., Moorwood, A. F. M., Lutz, D., Tielens, A. G. G. M., Siebenmorgen, R., Keane, J. V. 2004, A&A, 414, 873 (S04)
 Sturm, E., Lutz, D., Tran, D., Feuchtgruber, H., Genzel, R., Kunze, D., Moorwood, A. F. M., Thornley, M. D. 2000, A&A, 358, 481
 Swinbank, A. M., Smail, I., Chapman, S., Blain, A., Ivison, R., Keel, W. C. 2004, ApJ, 617, 64

Tran, Q. D. et al. 2001, ApJ, 552, 527
Voit, G. M. 1992, MNRAS, 258, 841
Webb, T. M. A., Lilly, S., Clements, D. L., Eales, S., Yun, M.,
Brodrin, M., Dunne, L., & Gear, W. 2003b, ApJ, 597, 680
Weedman, D. W., Le Floc'h, E., Higdon, S. J. U., Higdon, J. L.,
Houck, J. R. 2006, ApJ, 638, 613

Yan, L. et al. 2005, ApJ, 628, 604 (Y05)